

**BETTERMENT OF THE TRACTOR FRAME DESIGN
APPLYING COMPUTATIONAL MECHANICS APPROACH**

Masayuki Koike
Institute of Agricultural & Forest Engineering
University of Tsukuba
Tsukuba, Ibaraki 305, Japan

ABSTRACT

The shape optimization procedure applying finite element method was carried out for the specific purpose of analysis of a tractor chassis frame. Minimization of the mass as an objective function is executed under multiple constrained conditions of nodal displacements and stresses. The optimization process executions were succeeded in converging into single optimum solution. Although mass reduction and stress alleviation were attained by 40% and 26 to 34% respectively, the geometry of the shape is so complicated for fabrication that the refinement of the geometry is of necessity.

Key Word : Tractor, Chassis frame, Finite element method, Optimum design, Stress concentration, Optimality criteria method

I. INTRODUCTION

In technological computation, the first step to be done is to define specific design problem. Through choosing appropriate software in view of computational mechanics, any product concept may be generated in the computer. Based on this geometry data, the numerical data are created, and then input data are incorporated in the task. Taking into account the boundary, initial and external force conditions, a model can be presented in the computer. This model is needed to execute the structural computations utilizing the finite element method(FEM). If any problems are found, the model may be forwarded for further modification and succeeding re-evaluation. Current design approach described above briefly is a universally accepted one in the workshop as highly adapted technology.

In this paper, a longitudinal beam of tractor's chassis frame was adopted aiming to create its optimum shape applying the optimality criteria method. What is more, strength performance of the model was evaluated from both numerical and experimental standpoints.

II. MATERIALS AND METHODS

2.1 The computer system

The engineering workstation (EWS) used in this research includes 12Mbytes of main memory, 156Mbytes hard disk drive, 60Mbytes cartridge tape drive and 1.2Mbytes diskette drive. The operating system that runs in the EWS is the UTek, Tektronix version of UNIX.

2.2 NISA II

NISA (Numerically Integrated element for System Analysis) II¹¹ is a general purpose finite element program which can be applied in solving various problems encountered in engineering mechanics as shown in Fig. 1. NISOPT family of programs SECOPT, STROPT and SHAPE is the FEM programs integrated with NISA II, which is utilized as the main analysis module.

2.3 Shape optimization

SHAPE uses the Lagrange multiplier formulation to generate what is generally known as the optimality criteria method. Constraints on structural response quantities, such as nodal displacements and element stresses, can be written in the form necessary to set up these expressions. Also based on the quality of the new design, measured particularly in terms of its efficiency, SHAPE decides on whether to update the active set and re-solve the optimality criteria problem or to accept the design and continue into the next stage of optimization.

The next stage involves a series of intermediate designs based on a sensitivity approach similar to that used in obtaining the optimality criteria. The measure of design efficiency is the "virtual volume" obtained as the ratio of the material volume to the most critical factor to the constraint surface. Shape optimization without due regard for efficiency quickly embeds the design at an inferior local optimum (Fig. 3). Thus, at this stage, some of the previously removed elements are restored to the structure based on the results of sensitivity analyses.

This iterative intermediate design stage ends when the program selects one of the generated designs as the most efficient design. This completes one 'design step'.

The optimization process will continue until the user specified total number of iterations or design steps is satisfied. Execution will end earlier if the program is not able to improve upon the last most efficient design generated.

III. RESULTS AND DISCUSSION

3.1 General optimization analysis

A chassis frame (Fig. 2) is currently getting higher popularity in almost all types of tractors due to better design flexibility and structural advantages.

In this specific analysis, the longitudinal beam was evaluated to attain the stress constrained problem which restraints the maximum value of von Mises equivalent stress to be less than 25MPa, applying the general optimization mode of SHAPE module. The solution converged at the design step of 12, indicating greater amount of mass reduction from 7.666kg of initial shape to 1.925kg of optimized model as shown in Table 1.

The design process may be observed in Fig. 4. In this case, zero in terms of the number of iteration corresponds initial shape and likewise 1 to 10, 11 to 17 and 18 to 21 correspond 1, 2 and 3 of each design step respectively (Fig. 5). It is of interest to note that at the final stage of each design step, the elements of the proposed model was removed considerably. This process is repeated until the material volume and virtual volume indicate same value or 1.0 in terms of the minimization index. The achievement of this stress state is referred to as the fully stressed design and hence it suggests that all stresses of elements approach to the constrained value.

The initial shape and its optimized one can be seen in Fig. 6(a) and (b) respectively. Three downward arrows stand for the applied force while another three supporting and connecting positions are imposed by the freezing parts at the outset. As for the number of elements, it would be reduced from 3472 of the initial shape to 872 of the optimized one (i.e. 74.9% reduction). However, up to this process, the proposed shape itself is seemed to be rather rugged, unrealistic one.

To refine it, the boundary optimization mode is executed in adding the aesthetic components as shown in Fig. 6(c).

3.2 Boundary optimization analysis

Assuming that the maximum allowable value of von Mises equivalent stress is 100MPa, the number of iteration for the boundary optimization mode was suspended at 263. The mass of proposed model takes 1.572kg and 1.574kg at the computation before and after smoothing process (Table 1).

As can be seen in Figs. 7 and 8, the displacement patterns show similar trend each other indicating maximum deflection in the neighborhood of center portion. On the contrary, in the case of stress distribution pattern, stresses tend to scatter in a certain wider ranges confirming avoidance of so-called stress concent-

ration.

3.3 Experimental verification test

A model of optimized chassis frame was fabricated and tested in order to ascertain the computational results. Figs. 9 and 10 show the model and the set-up for the static, loading test. The difference of displacements for a specific position between numerical and experimental value is approximately less than 10%. Furthermore, stress distribution is found to follow similar trend for both of them.

IV. CONCLUSIONS

The optimization shape of chassis frame is found to satisfy the objective function in terms of the minimum mass design. It can be concluded that the model is needed to evaluate in seeking further refinement to attain easier manufacturing process, although superior enough in the strength reinforcement and mass reduction effect.

REFERENCES

1. Engineering Mechanics Research Corporation. 1989. NISAOPT user's manual. EMRC, P.O.Box 696, Troy, Michigan.
2. Koike, M., T. Konaka, T. Takigawa and T. Kaji. 1993. Numerical simulation using the engineering workstation -Application for the bush cutter and the ROPS -. Journal of the Japanese Society of Agricultural Machinery (in press).
3. Motobayashi, K., M. Koike and T. Konaka. 1992. Optimum design of the tractor members applying FEM(Part 1) -Linear static strength analysis for a toplink and a drawbar-. J. JSAM 54(4): 29-37.
4. Motobayashi, K., M. Koike and T. Konaka. 1993. Optimum design of the tractor members applying FEM(Part 2) -Shape optimization analysis for a chassis frame-. J. JSAM 55(4): 3-11.
5. Suministrado, D.C., M. Koike and T. Konaka. 1991. Numerical analysis of stress and strain on a moldboard plow bottom -Application of NISA II-. J. JSAM 53(5): 11-21.

Table 1 Comparison between optimization model and prototype

	Prototype	Initial shape	General optimization mode		Boundary optimization mode	
			Before smoothing	After smoothing	Before smoothing	After smoothing
Number of element	1616	3472	872	834	712	677
Number of nodal point	951	1875	692	686	533	530
Degree of freedom	1893	****	****	1291	1057	977
Volume ($\times 10^{-4} \text{ m}^3$)	4.410	9.765	2.453	2.546	2.003	2.006
Mass (kg)	3.462	7.666	1.925	1.999	1.572	1.575
Overall strain energy ($\times 10^{-2} \text{ N}\cdot\text{m}$)	9.403		10.570	8.577	30.160	23.167
Max. deflection of nodal point ($\times 10^{-5} \text{ m}$)						
x-direction	6.43 (663)		-8.98 (203)	-8.08 (194)	11.57 (184)	10.21 (184)
y-direction	-17.80 (1065)		-24.55 (384)	-20.20 (376)	-64.47 (276)	-51.03 (283)
Max. stress of nodal point (MPa)						
Max. principal stress	32.49 (542)		23.24 (428)	21.95 (447)	47.38 (134)	51.81 (293)
Min. principal stress	-37.55 (553)		-22.76 (418)	-24.97 (304)	-46.65 (135)	-47.77 (272)
Max shearing stress	18.78 (553)		11.62 (428)	12.54 (304)	23.69 (134)	26.05 (299)
von Mises equivalent stress	33.86 (536)		23.24 (428)	25.02 (304)	47.38 (134)	51.70 (299)

N.B.: Digit in the parenthesis stands for the corresponding nodal number.

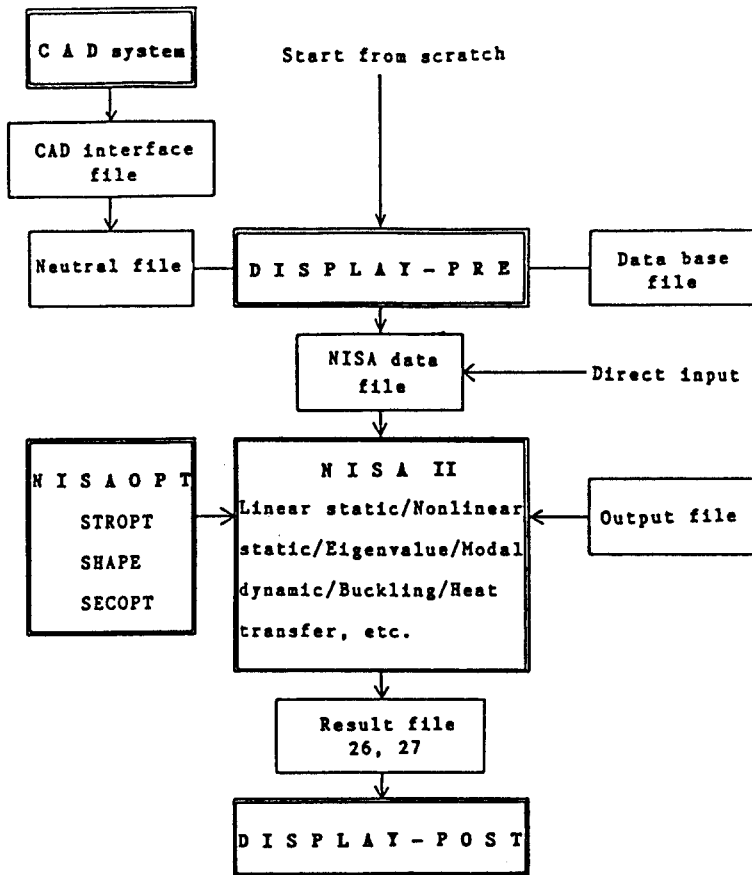


Fig. 1 Schematic diagram of the basic steps in FEM analysis with DISPLAY and NISA II programs

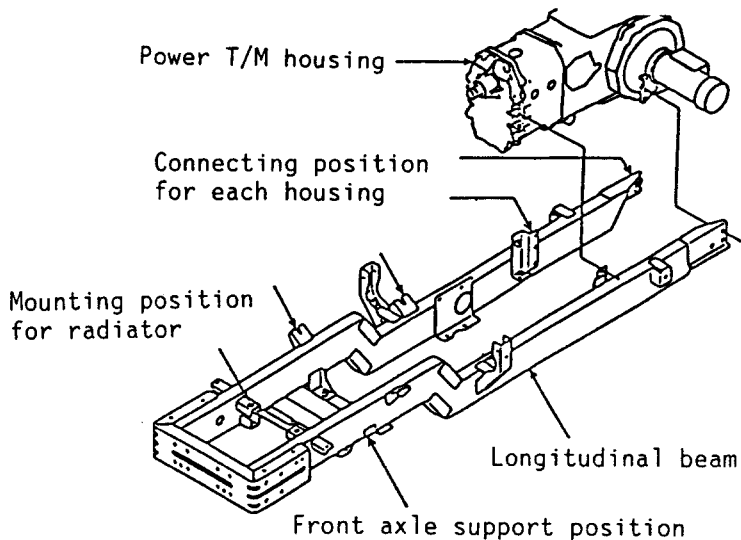


Fig. 2 A chassis frame of prototype

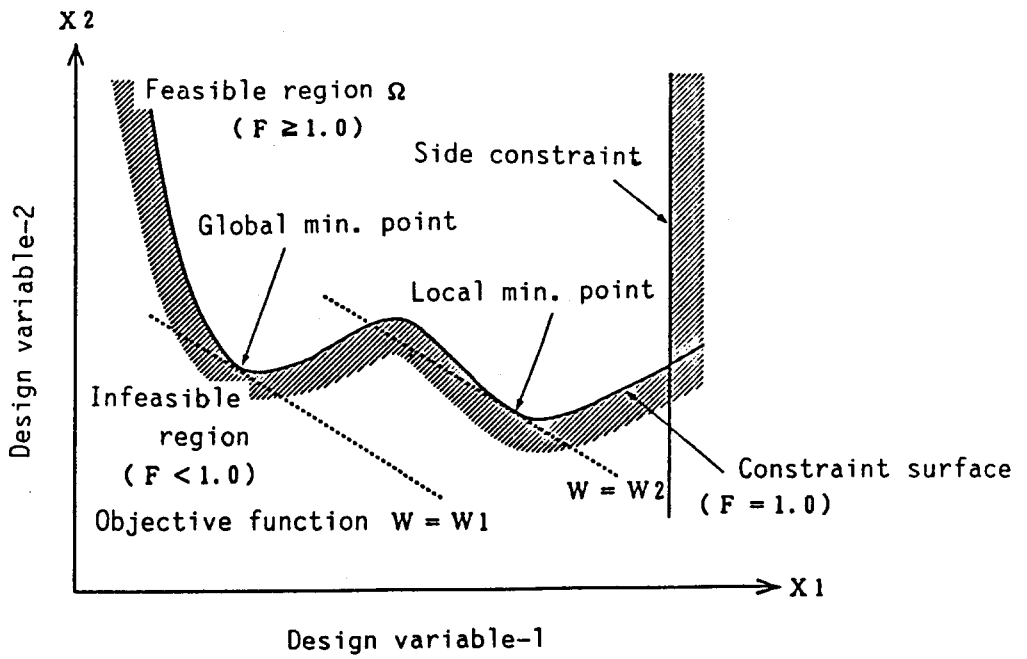


Fig. 3 Design space and objective function

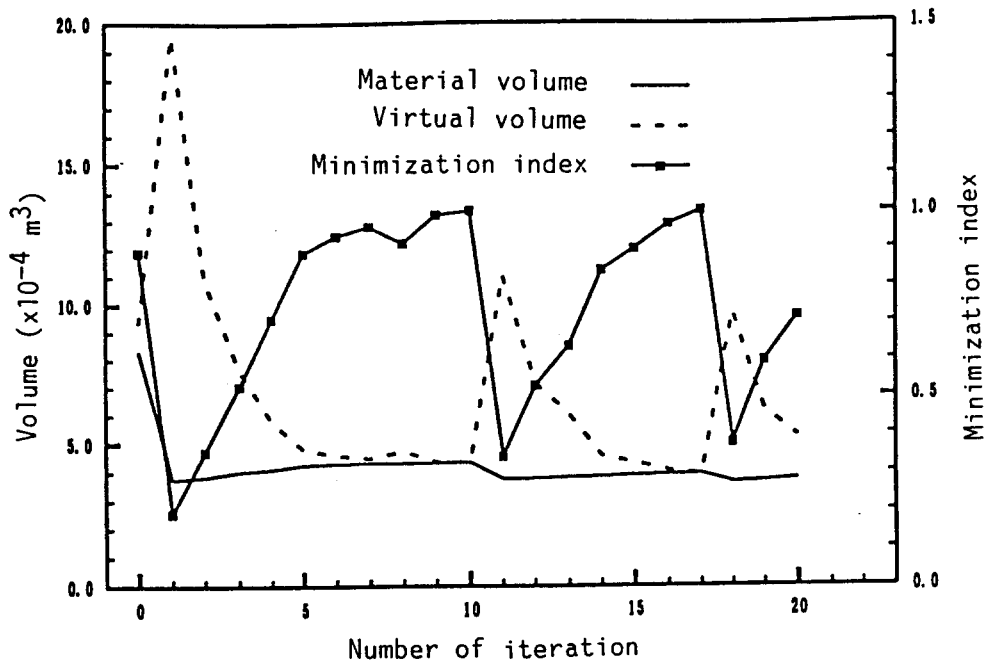


Fig. 4 Optimization process (In the case of the number of iteration from 0 to 20)

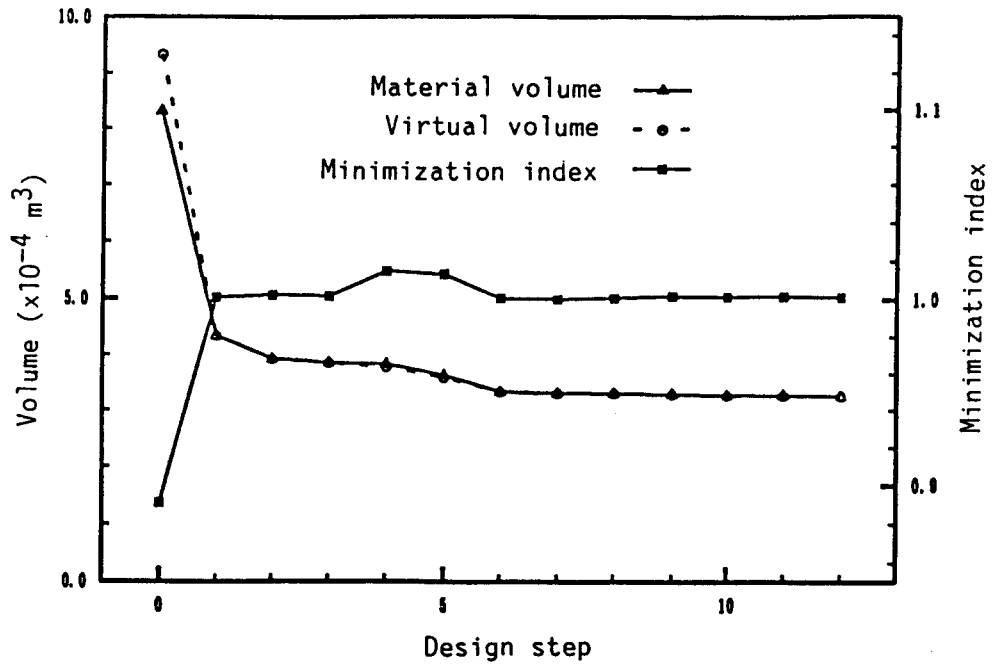


Fig. 5 Optimization process (In the case of the design step from 0 to 12)

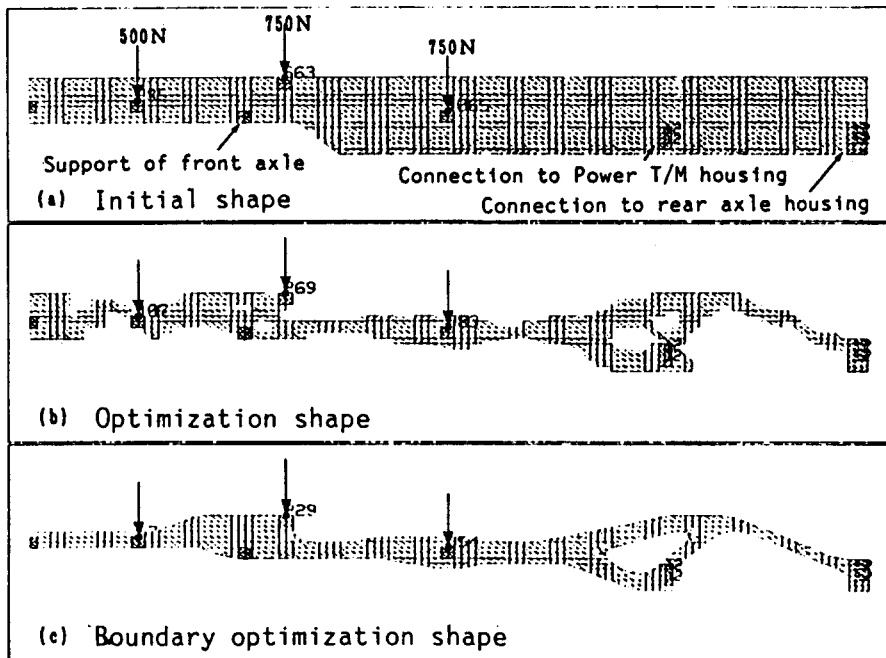


Fig. 6 Shape optimization of the model proposed

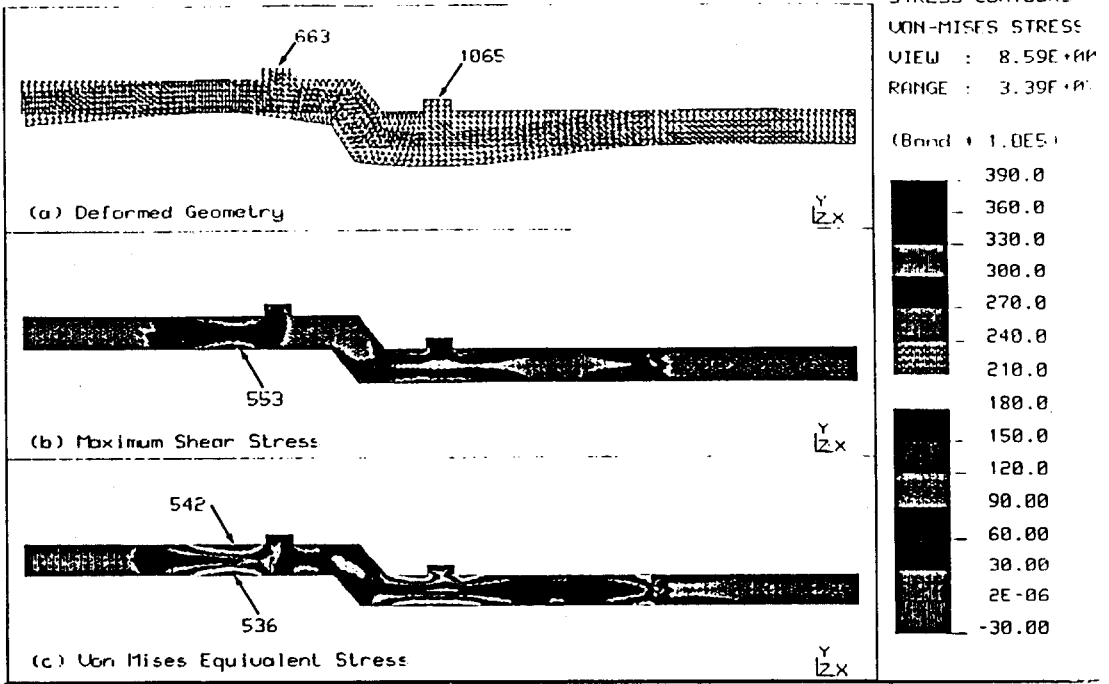


Fig. 7 Linear, static FEM analysis of prototype

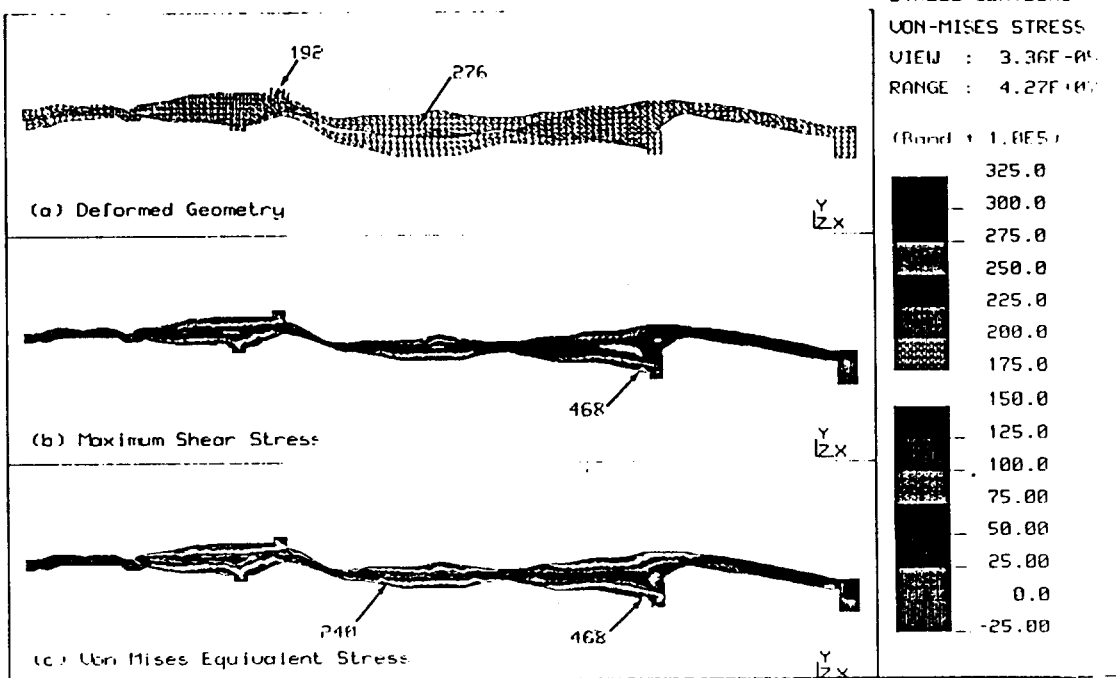


Fig. 8 Results of the boundary optimization analysis

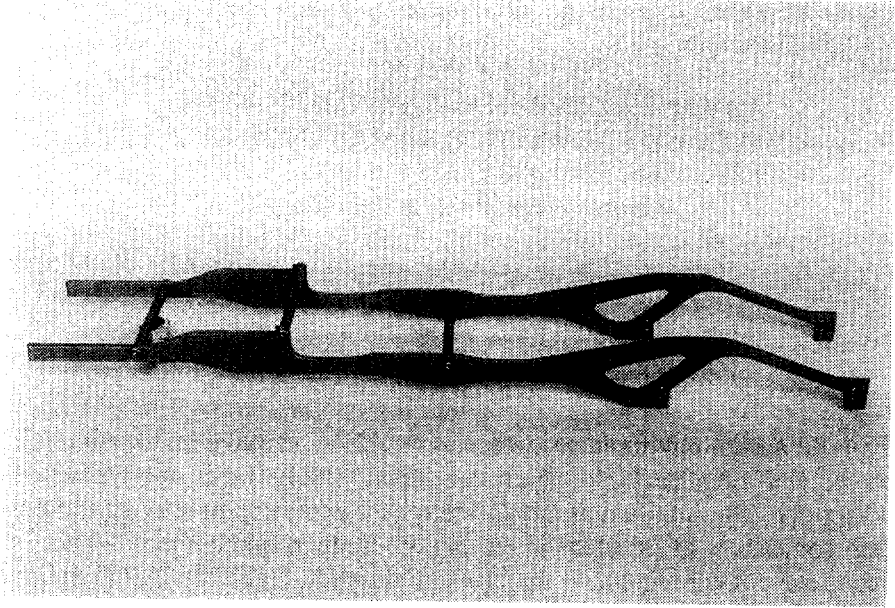


Fig. 9 A fabricated model which followed the shape optimization result

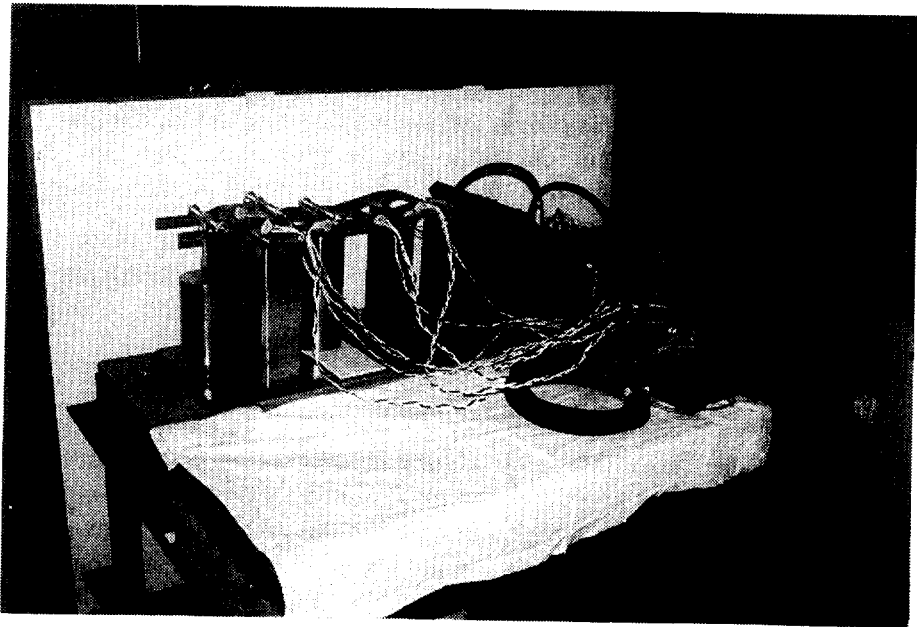


Fig. 10 Experimental set-up of the model frame for the verification test